

RAPIDITY DEPENDENCE OF THE CHARGED PARTICLE MULTIPLICITY DISTRIBUTIONS IN e^+e^- ANNIHILATION AT 29 GeV

M. DERRICK, K.K. GAN, P. KOOIJMAN, J.S. LOOS, B. MUSGRAVE, L.E. PRICE,
J. SCHLERETH, K. SUGANO, J.M. WEISS¹, D.E. WOOD²

Argonne National Laboratory, Argonne, IL 60439, USA

D. BLOCKUS, B. BRABSON, S.W. GRAY³, C. JUNG, H. NEAL, H. OGREN, D.R. RUST,
M. VALDATA-NAPPI⁴

Indiana University, Bloomington, IN 47405, USA

C. AKERLOF, G. BONVICINI, J. CHAPMAN, D. ERREDE, N. HARNEW⁵, P. KESTEN⁶,
D.I. MEYER, D. NITZ, A.A. SEIDL², R. THUN, T. TRINKO², M. WILLUTZKY

University of Michigan, Ann Arbor, MI 48109, USA

S. ABACHI, P. BARINGER, I. BELTRAMI⁷, B.G. BYLSMA, R. DEBONTE, D. KOLTICK,
F.J. LOEFFLER, E.H. LOW, R.L. McILWAIN, D.H. MILLER, C.R. NG, L.K. RANGAN,
E.I. SHIBATA

Purdue University, West Lafayette, IN 47907, USA

and

B. CORK

Lawrence Berkeley Laboratory, Berkeley, CA 94720, USA

Received 7 January 1986

The charged particle multiplicity distribution for e^+e^- annihilations at $\sqrt{s} = 29$ GeV has been measured using the High Resolution Spectrometer at PEP. The multiplicity distribution, expressed as a function of the mean, shows KNO scaling when compared to e^+e^- data at other energies. Multiplicity distributions for particles selected in different central rapidity spans are presented. All of these are well represented by the negative binomial distribution. As the rapidity span is narrowed, the distributions become broader and approach a constant value of the parameter k .

¹ Present address: SRI International, Menlo Park, CA 94025, USA.

² Present address: Lockheed Missiles and Space Co., Sunnyvale, CA 94806, USA.

³ Present address: Cornell University, Ithaca, NY 14853, USA.

⁴ Permanent address: INFN, I-56010 Pisa, Italy.

⁵ Present address: CERN, CH-1211 Geneva 23, Switzerland.

⁶ Present address: Brandeis University, Waltham, MA 02254, USA.

⁷ Present address: ETH, CH-8093 Zurich, Switzerland.

Measurements of charged particle multiplicity distributions in hadronic collisions have provided important constraints on models of multiparticle production^{†1}. This has been less true for the simpler case of e^+e^- annihilation since the available data have been sparse. The most striking feature of all data was the observation of a scaling behavior first suggested by

^{†1} See e.g. the recent review by Sukhatme [1].

Koba, Nielsen, and Olesen [2] (KNO). Specifically, if $z = n/\langle n \rangle$, then KNO scaling says that $\psi(z) = \langle n \rangle \sigma_n / \Sigma \sigma_n$ is a universal function for a given type of reaction, where $\langle n \rangle$ is the mean charged particle multiplicity, and σ_n is the cross section for producing events containing n charged particles. The scaling holds for hadronic reactions from an energy of a few GeV through the energy ranges of Fermilab and the ISR.

For the high energies of the CERN $\bar{p}p$ collider ($200 \text{ GeV} < \sqrt{s} < 900 \text{ GeV}$), the scaling breaks down [3], and a broader distribution is observed with many more high multiplicity events. These high energy data when restricted to the central region of pseudorapidity [4], also show a broader KNO distribution than is observed for the inclusive data sample.

In e^+e^- annihilation, KNO scaling is experimentally confirmed in the range $5 \text{ GeV} < \sqrt{s} < 34 \text{ GeV}$, but the distribution is narrower than that observed in the nondiffractive hadronic collisions [5]. This observation prompted Bialas and Hayot [6] to suggest that energy and momentum constraints may be responsible for suppressing the higher multiplicities in e^+e^- annihilation. This implies that the multiplicity distribution for tracks in the central rapidity region, well away from the kinematic boundary, could be wider than that observed for the unselected data.

In this paper we present new data on charged particle multiplicity distributions in e^+e^- annihilation. The distributions are studied as a function of the rapidity span of the charged tracks. The results were obtained from the hadronic annihilation events collected by the High Resolution Spectrometer (HRS) at the SLAC e^+e^- storage ring PEP. The experiment was done at a center-of-mass energy of 29 GeV and the data sample corresponds to an integrated luminosity of 185 pb^{-1} .

The HRS is a solenoidal spectrometer that measures charged particles and electromagnetic energy over 90% of the solid angle [7]. The tracking system consists of a vertex chamber, a central drift chamber, and an outer drift chamber. The central drift chamber has 15 layers of cylindrical drift planes, eight of which have stereo wires ($\pm 60 \text{ mrad}$) in order to measure the position along the e^+e^- beam direction. The momentum of a charged particle in the 1.62 T magnetic field is measured with a resolution of 3% at $14.5 \text{ GeV}/c$. The minimum momentum for detecting tracks with good efficiency is about $200 \text{ MeV}/c$. The 40-module

barrel shower counter system provides electromagnetic calorimetry over 62% of the solid angle with energy resolution of $\sigma_E/E = 0.16/\sqrt{E}$ (GeV).

The beam pipe and the inner wall of the central drift chamber are made of beryllium so as to minimize the conversion of photons into electron-positron pairs; the total material between the interaction point and the central drift chamber is less than 0.02 radiation lengths.

The events were selected to have m well reconstructed tracks where $5 \leq m < 40$. In addition, the sum of the charged particle momenta, plus the energy observed in the barrel shower counter, was required to be greater than 12 GeV , with at least 1 GeV in the shower counter and more than $7.5 \text{ GeV}/c$ in the scalar sum of the charged particle momenta. The invariant masses of three-prong jets in six-prong events was required to be greater than the τ lepton mass.

To ensure good tracking efficiency, the thrust axis of the event was selected to be within 30° of the equatorial plane of the detector, and each track had to have an angle with respect to the e^+e^- beam direction of more than 24° and had to register in more than one-half of the drift chamber layers traversed. With these selections, the reconstruction efficiency for isolated tracks was greater than 99%. For a typical annihilation event, with several close neighboring tracks, the reconstruction efficiency is 80% or better and varies slowly with dip angle; for the higher momenta, $p > 2 \text{ GeV}/c$, this efficiency increases to 90%.

In addition to this inclusive data set, a sample of two-jet events was selected using the sphericity and aplanarity variables. The criteria used were a sphericity less than 0.25 and an aplanarity less than 0.10. These cuts, which exclude the events with hard gluon radiation, give a data set of collimated and planar events. Most of the remaining background events, from two-photon interactions and beam gas scattering, are also removed by these selections. The inclusive (two-jet) data sample includes about 30 K (24 K) events.

The true multiplicity distribution was determined from the observed data by means of a matrix unfolding technique. If N_m^0 is the number of events observed with m tracks and N_n^T is the true number of events with n tracks (n even), we define M_{nm} such that

$$N_n^T = \sum_m M_{nm} N_m^0. \quad (1)$$

The matrix M_{nm} was determined from a Monte Carlo simulation of the experiment which includes the effects of the experimental cuts as well as the tracking inefficiencies. The matrices were calculated independently for all selected rapidity intervals and the results were found to be stable for reasonable variations, both of the cuts and of the definition of a good track. The number of events with $n < 5$ was estimated from the data, assuming independent fragmentation of the two jets. Events with no charged particle in the selected rapidity span were included in the data sample.

For the inclusive data sample, the charged particle multiplicity distribution in KNO form is shown in fig. 1 where it is compared to the published TASSO data [8]. The errors shown are statistical; the typical point-to-point systematic uncertainty for the present

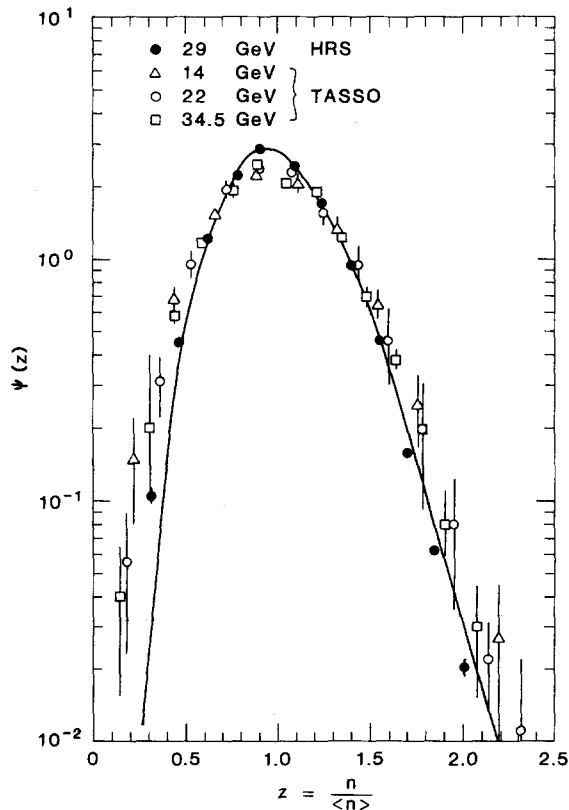


Fig. 1. Multiplicity distributions for e^+e^- annihilation expressed in KNO form. The statistical errors for the HRS data are smaller than the size of the full circles. The TASSO data is from ref. [8]. The line shows the fit to the HRS data using the gamma distribution of eq. (4).

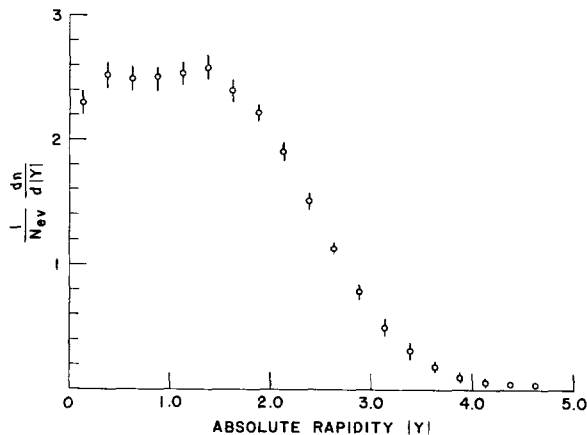


Fig. 2. Folded rapidity distribution measured along the thrust axis of the event. The errors are dominated by systematic uncertainties.

experiment is 4%. The agreement is satisfactory considering the errors, although our results indicate a somewhat narrower distribution, which is almost poissonian.

The folded rapidity distribution, where the rapidity is measured along the thrust axis of the event, extends over the range $|Y| \lesssim 4$, as seen in fig. 2. In calculating Y , all particles are assigned the pion mass. The statistical uncertainties on the data points are very small; the errors shown are dominated by the systematics. The kinematic limit is at $|Y| = 5.3$.

The KNO multiplicity distributions for the two-jet data sample and for particles contained in selected rapidity ranges from $|Y| < 0.1$ to $|Y| < 2.5$, corresponding to Y spans from 0.2 to 5.0 units, are shown in fig. 3. Each successive data set has been displaced lower by a factor of ten for clarity. The two-jet data with no Y selection are also shown with their own ordinate scale. These events are always even prongs so the normalization differs by a factor of two from that of the data with a rapidity selection. The distributions clearly widen as the rapidity span is restricted, and for $Y \lesssim 1$ events with z values of 3 to 5 are seen.

The multiplicity distributions for the data in the outer regions of the rapidity span has also been studied. In all cases, the distribution is narrow, even when the Y range selected is small.

The data of fig. 3 have been fitted to the negative binomial distribution

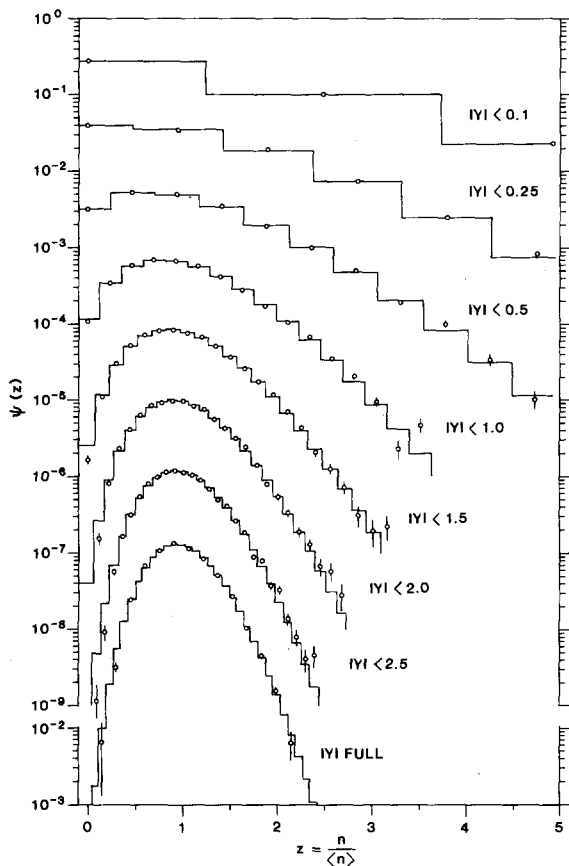


Fig. 3. Multiplicity distributions for two-jet events of e^+e^- annihilation at 29 GeV as a function of the rapidity span selection. The histograms show the best fit to the negative binomial of eq. (2) expressed in KNO form. Each of the selected distributions has been shifted down by a factor of ten relative to the $|Y| < 0.1$ data. The ordinate scale for the data set with no rapidity selection is shown separately.

$$P(n, \langle n \rangle, k) = \frac{k(k+1) \dots (k+n-1)}{n!} \times \left(\frac{\langle n \rangle / k}{1 + \langle n \rangle / k} \right)^n \left(1 + \frac{\langle n \rangle}{k} \right)^{-k} \quad (2)$$

In this parameterization, the shape of the distribution is determined by the parameter k and the position of the maximum by $\langle n \rangle$. The variable k is related to the mean multiplicity $\langle n \rangle$ and the dispersion D by

$$D^2 / \langle n \rangle^2 = 1 / \langle n \rangle + 1 / k. \quad (3)$$

The histograms in fig. 3 show the results of the fits to eq. (2). It is remarkable how well the negative binomial distribution represents the data. Including systematic errors, the typical χ^2 -per-degree of freedom is about unity for all of the data shown in fig. 3. In all cases, the value of k calculated from the measured values of D and $\langle n \rangle$ agrees to within a few percent with that given by the fit of the data to eq. (2).

The negative binomial expression, defined for integral values of n , can be derived assuming that the final state particles obey Bose-Einstein statistics [9]. According to these ideas, k can be thought of as the number of identical emitters or cells in phase space. However, since the fits to hadronic data [10] show a logarithmic increase of $1/k$ with \sqrt{s} , the number of independent emitters would be decreasing with energy, which is difficult to understand intuitively.

In the limit of $\langle n \rangle$ large compared to k , the negative binomial (2) leads to the gamma distribution:

$$\psi(z) = [K^K / \Gamma(K)] z^{K-1} \exp(-Kz). \quad (4)$$

The line in fig. 1 shows the fit of the HRS unselected data to this function. The resulting K value is 12.02. This form also fits the rapidity selected data with the value of K falling from 11 for $|Y| < 3$ to $K \sim 3$ for $|Y| < 1$.

However, the data in rapidity spans less than $|Y| = 1$ are not well represented by eq. (4) if the events with no tracks in the selected rapidity range are included. If these zero-prong events are discarded, then the gamma distribution provides good fits down to $|Y| < 0.5$ with $K = 2.5$ for this selection.

The values of k obtained by fitting the data of fig. 3 to the negative binomial are shown in fig. 4a, connected by the solid line. The k value falls rapidly as the Y limit is restricted but levels off for the central rapidity region at values of k between 5 and 10. The lower data set, connected by the dashed line, corresponds to the full data sample without the two-jet selection. The overall variation with Y is similar for the two data sets. Fig. 4b shows the (two-jet) mean charged particle multiplicities (scale on left) and dispersion values (scale on right) for the different Y selections. The lines are drawn to guide the eye.

The variation of k with Y , shown in fig. 4a, differs qualitatively from the observation of the UA5 group [5] who studied $\bar{p}p$ interactions at $\sqrt{s} = 540$ GeV and found a continuous broadening of the multiplicity

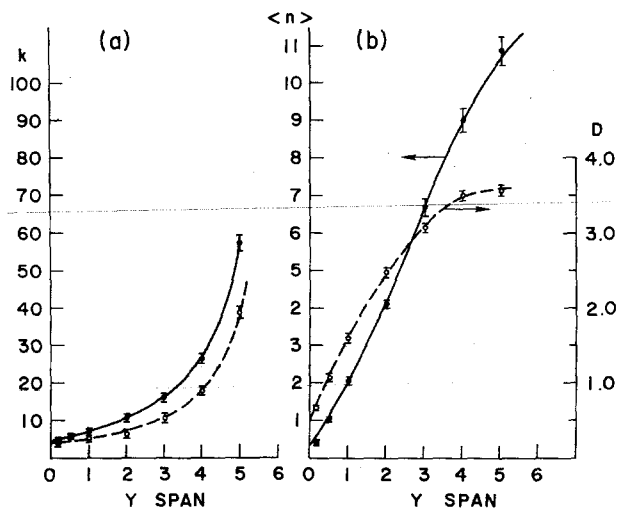


Fig. 4. (a) Fitted values of k as a function of rapidity span for the two-jet data of fig. 3 (upper data set). The lower data set connected by the dashed line shows the corresponding k values for the data sample without the two-jet selection. (b) Mean charged particle multiplicity, $\langle n \rangle$ (scale on the left), and dispersion, D (scale on the right) as a function of rapidity span for the two-jet data. The lines connecting the data points are drawn to guide the eye.

distribution as the pseudorapidity range was narrowed: no tendency to a limiting shape was seen. However, the $\bar{p}p$ distributions are broader, characterized by k values falling from ~ 3.8 to 1.5 as the pseudorapidity span is restricted.

Bialas and Hayot [6] have fitted the TASSO data [8] for the full rapidity range in a model with independent emission of clusters; they predict a limiting KNO distribution for the central rapidity region with K values for the gamma distribution representation of 2 to 3. This expectation is supported by our data and so may be taken to confirm the dominant role of energy and momentum conservation in narrowing the e^+e^- KNO distribution for the full rapidity span. The narrow multiplicity distribution observed for the data in the outer rapidity spans also supports this conclusion.

Many possible explanations for the origin of the negative binomial and the gamma distributions have been given. Expressions giving similar KNO shapes can be derived from a generating function which describes the QCD branching processes underlying the

evolution of the final state at the parton level [11]. Some authors have also advocated the idea of partial coherence between the emitters as the source of the breakdown of KNO scaling observed for hadronic collisions [12]. As is clear from fig. 4b, our mean charged multiplicity values are smaller than the k values, and so the requirement that $\langle n \rangle \gg k$ is not satisfied. However, the gamma distribution fits the data in the wider rapidity spans reasonably well as exemplified by the line in fig. 1. The negative binomial distribution gives a good representation of all of the data and so both expressions can be considered as good parameterizations in search of a physical explanation.

Since the basic partonic processes responsible for e^+e^- annihilation are much simpler than for hadronic collisions, particularly in the central rapidity interval, the observations reported here offer a more elementary challenge to theoretical understanding. The e^+e^- data are also free of complications arising from leading particle effects and diffractive processes that add ambiguity to the meaning of the hadronic data.

One interesting possibility is connected with the long outstanding observation that the data on rapidity correlations can be understood in terms of the emission of clusters that subsequently decay to give the observed hadrons [13]. The e^+e^- data show similar effects [14] with a typical correlation length of one unit of rapidity and a total multiplicity per cluster of 2–3 particles. The central region would then contain hadrons from the decay of a few clusters, irrespective of the Y cut, as long as it is comparable to the correlation length.

Several authors [15,16] have interpreted the hadronic data on such a model. Giovannini and Van Hove [15] have also considered the implications for e^+e^- annihilation, and, in a cascade model, the cluster charged particle multiplicity, $\langle n \rangle_c$, is controlled by a parameter $b = \langle n \rangle / (\langle n \rangle + k)$ being given by

$$\langle n \rangle_c = \frac{b}{b-1} \frac{1}{\ln(1-b)}.$$

The present results give b values in the range 0.15 to 0.3 as the rapidity span is changed corresponding to $\langle n \rangle_c$ values between 1.1 and 1.2. The 540 GeV $\bar{p}p$ data by contrast gives $\langle n \rangle_c \sim 3$ when interpreted in this model [15].

This work was supported in part by the US Depart-

ment of Energy, under Contracts W-31-109-Eng-38, DE-AC02-76ER01112, DE-AC03-76SF00098, DE-AC02-76ER01428, and DE-AC02-84ER40125. We thank L. Van Hove and P. Carruthers for interesting correspondence.

References

- [1] U.P. Sukhatme, UIC 85-15, in: Proc. XVI Symp. on Multiparticle dynamics (1985), to be published.
- [2] Z. Koba, H.B. Nielsen and P. Olesen, Nucl. Phys. B40 (1972) 317.
- [3] UA5 Collab., G.J. Alner et al., Phys. Lett. 138B (1985) 304.
- [4] UA5 Collab., G.J. Alner et al., Phys. Lett. 160B (1985) 193.
- [5] M. Derrick, Multiplicities in high energy interactions, ANL-HEP-CP-85-17, Proc. 1985 Aspen Winter School.
- [6] A. Bialas and F. Hayot, Phys. Rev. D33 (1986) 39.
- [7] D. Bender et al., Phys. Rev. D30 (1984) 515.
- [8] TASSO Collab., M. Althoff et al., Z. Phys. C22 (1984) 307.
- [9] A. Giovannini, Nuovo Cimento 15A (1973) 543; W.J. Knox, Phys. Rev. D10 (1974) 65; P. Carruthers and C.C. Shih, Phys. Lett. 127B (1983) 242.
- [10] UA5 Collab., G.J. Alner et al., Phys. Lett. 160B (1985) 199.
- [11] B. Durand and S.D. Ellis, Proc. 1984 Summer Study on the Design and utilization of the superconducting super collider, eds. J. Morfin and R. Donaldson (Snowmass, CO, 1984) p. 234.
- [12] M. Biyajima, Phys. Lett. 137B (1984) 225; P. Carruthers and C.C. Shih, Phys. Lett. 137B (1984) 425; M. Blazek, Z. Phys. C26 (1984) 455; G.N. Fowler et al., Marburg preprint (1985).
- [13] See e.g. G. Giacomelli and M. Jacob, Phys. Rep. 55 (1979) 1.
- [14] W. Koch, Proc. XIII Symp. on Multiparticle dynamics, eds. W. Kittel, W. Metzger and A. Stergiou (1982) p. 534; M. Valdata-Nappi, Proc. XIV Symp. on Multiparticle dynamics, eds. P. Yager and J.F. Gunion (1983) p. 75.
- [15] A. Giovannini and L. Van Hove, Negative binomial multiplicity distributions in high energy hadron collisions, CERN TH-4230/85 (1985).
- [16] C.S. Lam and H.S. Zahir, Multiplicity distributions in limited pseudorapidity intervals, McGill preprint (1985).